ROBUST RESIDUAL-BASED A POSTERIORI ARNOLD–WINTHER MIXED FINITE ELEMENT ANALYSIS IN ELASTICITY*

CARSTEN CARSTENSEN AND JOSCHA GEDICKE

ABSTRACT. This paper presents a residual-based a posteriori error estimator for the Arnold–Winther mixed finite element that utilises a post-processing for the skew-symmetric part of the strain. Numerical experiments verify the proven reliability and efficiency for suitable approximation of the skew-symmetric deformation gradient. Numerical evidence supports that the L^2-stress error estimator is robust in the Poisson ratio and allows stable error control even in the incompressible limit.

1. INTRODUCTION

The problem in linear elasticity considers the connected reference configuration of the elastic body $\Omega \subset \mathbb{R}^2$ with polygonal boundary $\partial\Omega = \Gamma_D \cup \Gamma_N$ with closed and connected Γ_D of positive surface measure and $\Gamma_N = \partial\Omega \backslash \Gamma_D$ for applied tractions. Given a volume force $f : \Omega \to \mathbb{R}^2$, a displacement $u_D : \Gamma_D \to \mathbb{R}^2$, and a traction $g : \Gamma_N \to \mathbb{R}^2$, find a displacement $u : \Omega \to \mathbb{R}^2$ and a stress tensor $\sigma : \Omega \to \mathbb{S} := \{\tau \in \mathbb{R}^{2\times 2} : \tau = \tau^T\}$ such that

$$\begin{aligned} -\operatorname{div}\sigma = f, \quad \sigma = \mathbb{C}\varepsilon(u) \quad \text{in } \Omega, \\ u = u_D \quad \text{on } \Gamma_D, \quad \sigma\nu = g \quad \text{on } \Gamma_N. \end{aligned} \tag{1.1}$$

Throughout this paper, $\mathbb{C}$ denotes the bounded and positive definite fourth-order elasticity tensor for isotropic linear elasticity. The symmetric mixed finite element method is a very popular choice for a robust stress approximation; cf. [AW02, BBF13, Bra01, BS94, CEG11, CGS15] for details and related references.

Key words and phrases. finite element method, Arnold–Winther, a posteriori error analysis, robustness, elasticity.

*The work of the first author has been supported through the German Science Foundation (DFG) through the research group FOR 797 "Analysis and Computation of Microstructures in Finite Plasticity" project CA151/19 and the Priority Programme (SPP) 1748 project CA151/22. The work of the second author was supported by a fellowship within the Postdoc-Program of the German Academic Exchange Service (DAAD).

Published in Comput. Methods Appl. Mech. Engrg. 300 (2016) 245–264. Available online at www.sciencedirect.com, http://dx.doi.org/10.1016/j.cma.2015.10.001.

The a posteriori error analysis for the Arnold–Winther finite element method may follow the ideas of [CD98, Car05, CH07] to derive a stress error control

$$||\sigma - \sigma_{AW}||^2_{\mathbb{C}^{-1}} \leq \min_{v\in V} ||\mathbb{C}^{-1}\sigma_{AW} - \varepsilon(u_D + v)||^2_{\mathbb{C}} + C_1\mathrm{osc}^2(f,\mathcal{T}) + C_2\mathrm{osc}^2(g,\mathcal{E}(\Gamma_N))$$

for the stress error $\sigma - \sigma_{AW}$ even with a rather explicit estimate of the constant in front of the oscillations and the (unwritten) multiplicative constant 1 in front of the first term that measures the quality of the approximation $\mathbb{C}^{-1}\sigma_{AW}$ of symmetric gradients $\varepsilon(v) := (Dv + D^T v)/2$ for $v \in V$. The space V consists of all square-integrable displacements with homogeneous boundary conditions along Γ_D and with a square-integrable functional matrix Dv.

A severe additional difficulty of this approximation is that only the symmetric part is approximated and not the full gradient Dv so that [CH07] cannot be applied for a residual-based a posteriori error estimation of the aforementioned first term. Other mixed finite element schemes like PEERS in [CD98] involve some additional variable to approximate the asymmetric part of the gradient. This paper presents an explicit error estimate which involves an arbitrary asymmetric approximation γ_h and provides an abstract a posteriori error control of the residual type, which is useful for adaptive mesh-refining algorithms,

$$\begin{aligned}\eta_\ell^2 &= \mathrm{osc}^2(f,\mathcal{T}) + \mathrm{osc}^2(g,\mathcal{E}(\Gamma_N)) \\ &\quad + \sum_{T\in\mathcal{T}} h_T^2 \|\mathrm{curl}(\mathbb{C}^{-1}\sigma_{AW} + \gamma_h)\|^2_{L^2(T)} \\ &\quad + \sum_{E\in\mathcal{E}(\Omega)} h_E \|[\mathbb{C}^{-1}\sigma_{AW} + \gamma_h]_E \tau_E\|^2_{L^2(E)} \\ &\quad + \sum_{E\in\mathcal{E}(\Gamma_D)} h_E \|(\mathbb{C}^{-1}\sigma_{AW} + \gamma_h - Du_D)\tau\|^2_{L^2(E)}.\end{aligned}$$

(The details on the standard notation can be found below for computable volume contributions on a triangle T of diameter h_T and various jumps across an edge E of length h_E.) For any (piecewise smooth) choice of γ_h, this a posteriori error estimator is reliable in the sense that

$$\|\sigma - \sigma_{\mathrm{AW}}\|_{\mathbb{C}^{-1}} \leq C_{\mathrm{rel}}\eta_\ell \tag{1.2}$$

with some λ-independent constant $C_{\mathrm{rel}} \approx 1$. One opportunity to ensure efficiency is a global minimisation over all piecewise polynomial γ_h of the error estimator η_ℓ. The bubble function technique shows that the particular choice of γ_h enters the efficiency estimates with some λ-independent constant $C_{\mathrm{eff}} \approx 1$,

$$\eta_\ell \leq C_{\mathrm{eff}} \left(\|\sigma - \sigma_{\mathrm{AW}}\|_{\mathbb{C}^{-1}} + \|\mathrm{skew}(Du) - \gamma_h\|_{L^2(\Omega)} \right). \tag{1.3}$$

Hence, one efficient choice for γ_h is to choose it as a sufficiently accurate polynomial approximation of the asymmetric gradient $\operatorname{skew}(Du) := (Du - D^T u)/2$. Since a global approximation or even minimisation may be too costly, this paper proposes to apply a post-processing step to compute such a sufficiently accurate approximation $\gamma_h = \operatorname{skew}(Du^*_{AW})$ for the post-processed displacement u^*_{AW} in the spirit of Stenberg [Ste88]. The approximation $\gamma_h = \operatorname{skew}(Du^*_{AW})$ is proven to be robust in the Poisson ratio $\nu \to 1/2$ for sufficiently smooth functions. For domains with re-entrant corners or incompatible boundary conditions, numerical experiments confirm that the proposed computation of γ_h leads empirically to reliable and efficient a posteriori error control independent of the Poisson ratio $\nu \to 1/2$.

The remaining parts of this paper are organised as follows. In Section 2 the notation, the weak formulation of (1.1) and the Arnold–Winther finite element space [AW02] are defined. Section 3 derives the a posteriori error analysis for the residual-based a posteriori error estimator and proves reliability and efficiency. Section 4 outlines a post-processing of the displacement that leads to an approximation γ_h of the asymmetric gradient. Section 5 presents numerical results of four benchmark problems that verify reliability and efficiency of the residual-based a posteriori error estimator in combination with the post-processing and illustrates its robustness for Poisson ratio $\nu \to 1/2$.

The main parts of this research are restricted to 2D because the Argyris finite element method is employed to allow for a quasi-interpolation in the Arnold–Winther finite element functions.

2. Preliminaries

For $v = (v_1, v_2) \in \mathbb{R}^2$ and $\tau = (\tau_{jk})_{j,k=1,2} \in \mathbb{R}^{2\times 2}$, set

$$\operatorname{Curl}(v) := \begin{pmatrix} \partial v_1/\partial y & -\partial v_1/\partial x \\ \partial v_2/\partial y & -\partial v_2/\partial x \end{pmatrix},$$

$$\operatorname{curl}\tau := \begin{pmatrix} \partial\tau_{12}/\partial x - \partial\tau_{11}/\partial y \\ \partial\tau_{22}/\partial x - \partial\tau_{21}/\partial y \end{pmatrix}, \quad \operatorname{div}\tau := \begin{pmatrix} \partial\tau_{11}/\partial x + \partial\tau_{12}/\partial y \\ \partial\tau_{21}/\partial x + \partial\tau_{22}/\partial y \end{pmatrix}.$$

Standard notation on Lebesgue and Sobolev spaces and norms is adopted throughout this paper and, for brevity, $\|\cdot\| := \|\cdot\|_{L^2(\Omega)}$ denotes the L^2 norm. In addition to the spaces $V := \{v \in H^1(\Omega;\mathbb{R}^2) \,\big|\, v|_{\Gamma_D} = 0\}$ and $H(\operatorname{div},\Omega) := \{q \in L^2(\Omega;\mathbb{R}^2) \,\big|\, \operatorname{div} q \in L^2(\Omega)\}$ set

$$H(\operatorname{div},\Omega;\mathbb{S}) := \{\tau \in L^2(\Omega;\mathbb{S}) \,\big|\, \operatorname{div}\tau \in L^2(\Omega;\mathbb{R}^2)\},$$

$$\Sigma_0 := \Big\{\sigma \in H(\operatorname{div},\Omega;\mathbb{S}) \,\Big|\, \int_{\Gamma_N} \psi\cdot(\sigma\nu)\,ds = 0 \text{ for all } \psi \in \mathcal{D}(\Gamma_N;\mathbb{R}^2)\Big\},$$

$$\Sigma_g := \Big\{\sigma \in H(\mathrm{div},\Omega;\mathbb{S}) \;\Big|\; \int_{\Gamma_N} \psi\cdot(\sigma\nu)\,ds = \int_{\Gamma_N}\psi\cdot g\,ds \text{ for all } \psi\in\mathcal{D}(\Gamma_N;\mathbb{R}^2)\Big\},$$

where the last two spaces involve the traction boundary conditions for $g \in L^2(\Gamma_N;\mathbb{R}^2)$ and $\mathcal{D}$ denotes the space of test functions. Let $\mathbb{M}^{2\times2}_{\mathrm{skew}} := \{\tau\in\mathbb{R}^{2\times2} : \tau = -\tau^T\}$ and let $\mathbb{S}$ denote the symmetric 2×2 matrices.

The dual weak formulation of (1.1) reads: Given data $u_D \in H^1(\Omega;\mathbb{R}^2)$, $f\in L^2(\Omega;\mathbb{R}^2)$, and $g\in L^2(\Gamma_N;\mathbb{R}^2)$, seek the solution $(\sigma,u)\in\Sigma_g\times L^2(\Omega;\mathbb{R}^2)$ with

$$\begin{aligned}\int_\Omega \sigma:\mathbb{C}^{-1}\tau\,dx + \int_\Omega u\cdot\mathrm{div}\,\tau\,dx &\\ = \int_{\Gamma_D} u_D\cdot(\tau\nu_\Omega)\,ds \quad &\text{for all } \tau\in\Sigma_0,\\ \int_\Omega v\cdot\mathrm{div}\,\sigma\,dx = -\int_\Omega f\cdot v\,dx \quad &\text{for all } v\in L^2(\Omega;\mathbb{R}^2).\end{aligned} \tag{2.1}$$

Let $\mathcal{T}$ be a shape-regular triangulation of $\overline{\Omega}$ into triangles with the set of interior edges $\mathcal{E}(\Omega)$, the sets of Dirichlet and Neumann boundary edges $\mathcal{E}(\Gamma_D)$ and $\mathcal{E}(\Gamma_N)$, and the set of nodes $\mathcal{N}$. For any triangle $T\in\mathcal{T}$, let $\mathcal{E}(T)$ be the set of its edges and h_T denotes the diameter of T. For any edge $E\in\mathcal{E}(T)$, let $\tau_E = (-n_2,n_1)^t$ be the unit tangential vector along E for the unit outward normal $\nu_E = (n_1,n_2)^t$ to E with the diameter h_E. The jump $[w]_E$ of w across $E = \overline{T}_+\cap\overline{T}_-$ reads

$$[w]_E := (w|_{T_+})|_E - (w|_{T_-})|_E.$$

This applies to an interior edge, written $E\in\mathcal{E}(\Omega)$, with edge-patch ω_E as the interior of $T_+\cup T_- = \overline{\omega_E}$. (The jump term along the boundary will be specified when it arises.)

Throughout this paper, $A\lesssim B$ abbreviates the inequality $A\le CB$ for some constant C that does neither depend on the mesh-sizes nor on λ but only on some lower bound of the minimal interior angle in the triangulation $\mathcal{T}$ and on μ.

The piecewise action of a differential operator is denoted with a subindex h, e.g., ∇_h denotes the piecewise gradient $(\nabla_h\cdot)|_T := \nabla(\cdot|_T)$ for all $T\in\mathcal{T}$.

The finite element spaces associated with the regular triangulation $\mathcal{T}$ of Ω into triangles involve the Arnold–Winther finite element $AW_k(\mathcal{T})$ of index $k\ge1$ [AW02] and the set $P_k(\mathcal{T};\mathbb{R}^{n\times m})$ and read

$$\begin{aligned}P_k(\mathcal{T};\mathbb{R}^{n\times m}) := \big\{v\in L^2(\Omega;\mathbb{R}^{n\times m}) \,\big|\, &v_{j,k}|_T \text{ is polynomial of total degree}\\ &\text{at most } k \text{ for all } T\in\mathcal{T}, 1\le j\le n, 1\le k\le m\big\},\\ AW_k(\mathcal{T}) := \big\{\tau\in P_{k+2}(\mathcal{T};\mathbb{S}) \,\big|\, &\mathrm{div}\,\tau\in P_k(\mathcal{T};\mathbb{R}^2)\big\},\end{aligned}$$

$$\Sigma_{0,h} := \Sigma_0 \cap AW_k(\mathcal{T}), \quad \Sigma_{g,h} := \Sigma_g \cap AW_k(\mathcal{T}), \quad V_h := P_k(\mathcal{T};\mathbb{R}^2).$$

The space $AW_k(\mathcal{T})$ consists of all symmetric polynomial matrix fields of degree $\leq k+1$ together with the divergence-free matrix fields of degree $\leq k+2$.

The mixed finite element method seeks $\sigma_{AW} \in \Sigma_{g,h}$ and $u_{AW} \in V_h$ such that

$$\begin{aligned} \int_\Omega \sigma_{AW} : \mathbb{C}^{-1}\tau_{AW}\,dx + \int_\Omega u_{AW} \cdot \operatorname{div} \tau_{AW}\,dx & \\ = \int_{\Gamma_D} u_D \cdot (\tau_{AW}\nu)\,ds \quad & \text{for all } \tau_{AW} \in \Sigma_{0,h}, \\ \int_\Omega v_h \cdot \operatorname{div} \sigma_{AW}\,dx = \int_\Omega f \cdot v_h\,dx \quad & \text{for all } v_h \in V_h. \end{aligned} \tag{2.2}$$

Theorem 2.1 ([AW02])**.** *The exact solution* $(\sigma, u) \in (\Sigma_g \cap H^{k+2}(\Omega;\mathbb{S})) \times H^{k+2}(\Omega)$ *of problem* (1.1) *and the approximate solution* (σ_{AW}, u_{AW}) *of problem* (2.2) *satisfy*

$$\begin{aligned} \|\sigma - \sigma_{AW}\|_{L^2(\Omega)} &\lesssim h^m \|\sigma\|_{H^m(\Omega)} \quad \textit{for } 1 \leq m \leq k+2, \\ \|\operatorname{div}(\sigma - \sigma_{AW})\|_{L^2(\Omega)} &\lesssim h^m \|\operatorname{div}\sigma\|_{H^m(\Omega)} \quad \textit{for } 0 \leq m \leq k+1, \\ \|u - u_{AW}\|_{L^2(\Omega)} &\lesssim h^m \|u\|_{H^{m+1}(\Omega)} \quad \textit{for } 1 \leq m \leq k+1. \quad \square \end{aligned}$$

3. Residual-based a posteriori error analysis

3.1. **Orthogonal error split.** For $v \in V := \{v \in H^1(\Omega) \,|\, v = 0 \text{ on } \Gamma_D\}$, define the residual by

$$\operatorname{Res}(v) := \int_\Omega f \cdot v\,dx + \int_{\Gamma_N} g \cdot v\,ds - \int_\Omega \sigma_{AW} : \varepsilon(v)\,dx$$

with its dual norm

$$|\!|\!|\operatorname{Res}|\!|\!|_* := \sup_{\substack{v \in V \\ |\!|\!|v|\!|\!| = 1}} \operatorname{Res}(v)$$

with respect to the energy norm

$$|\!|\!|v|\!|\!|^2 := \int_\Omega \varepsilon(v) : \mathbb{C}\varepsilon(v)\,dx.$$

Let

$$\|\tau\|^2_{\mathbb{C}^{-1}} := \int_\Omega \tau : \mathbb{C}^{-1}\tau\,dx$$

and

$$\operatorname{dist}^2_{\mathbb{C}}(\mathbb{C}^{-1}\tau, \varepsilon(u_D + V)) := \min_{w \in u_D + V} \|\mathbb{C}^{-1}\tau - \varepsilon(w)\|^2_{\mathbb{C}}.$$

Theorem 3.1. *The exact (resp. discrete) stress field* σ *(resp.* σ_{AW}*) satisfies*

$$\|\sigma - \sigma_{AW}\|^2_{\mathbb{C}^{-1}} = |\!|\!|\operatorname{Res}|\!|\!|^2_* + \operatorname{dist}^2_{\mathbb{C}}(\mathbb{C}^{-1}\sigma_{AW}, \varepsilon(u_D + V)).$$

Despite that Ω is a bounded domain in $\mathbb{R}^2$ with polygonal boundary, the (relative) open part Γ_N of the boundary $\Gamma := \partial\Omega$ is supposed to have a finite number of connected components $\Gamma_0, \ldots, \Gamma_J$, and Γ_D of positive surface measure is closed and connected.

Proposition 3.2 (Helmholtz decomposition [CD98, Lemma 3.2])**.** *Given any $\sigma - \sigma_{AW} \in L^2(\Omega;\mathbb{S})$, there exists $a \in \{v \in H^1(\Omega;\mathbb{R}^2) : v = 0 \text{ on } \Gamma_D\}$ and $\beta \in \{\phi \in H^2(\Omega) : \int_\Omega \phi\,dx = 0, \operatorname{Curl}\phi = c_j \in \mathbb{R}^2 \text{ on } \Gamma_j \subseteq \Gamma_N, j = 0, \ldots, J, c_0 = 0\}$ such that*

$$\sigma - \sigma_{AW} = \mathbb{C}\varepsilon(a) + \operatorname{Curl}\operatorname{Curl}\beta. \quad \square \tag{3.1}$$

Proof of Theorem 3.1. The Helmholtz decomposition of Proposition 3.2 leads to some unique $a \in V$ and $\beta \in H^2(\Omega) \cap L^2_0(\Omega)$ for which $\operatorname{Curl}\beta$ equals a constant c_j on Γ_j for any $j = 0, \ldots, J$ with $c_0 := 0$. The decomposition (3.1) is orthogonal with respect to the L^2 scalar product when weighted by $\mathbb{C}^{-1}$, i.e.,

$$\|\sigma - \sigma_{\mathrm{AW}}\|^2_{\mathbb{C}^{-1}} = |\!|\!|a|\!|\!|^2 + \|\operatorname{Curl}\operatorname{Curl}\beta\|^2_{\mathbb{C}^{-1}}.$$

For any $v \in V$ with $|\!|\!|v|\!|\!| = 1$, an integration by parts with the exact stress field $\sigma := \mathbb{C}\varepsilon(u)$ shows

$$\mathrm{Res}(v) = \int_\Omega (\sigma - \sigma_{\mathrm{AW}}) : \varepsilon(v)\,dx.$$

This implies

$$\mathrm{Res}(v) = \int_\Omega \mathbb{C}\varepsilon(a) : \varepsilon(v)\,dx \le |\!|\!|a|\!|\!|,$$

and so

$$|\!|\!|\mathrm{Res}|\!|\!|_* \le |\!|\!|a|\!|\!|.$$

Conversely,

$$|\!|\!|a|\!|\!|^2 = \mathrm{Res}(a) \le |\!|\!|\mathrm{Res}|\!|\!|_* |\!|\!|a|\!|\!|.$$

Altogether,

$$|\!|\!|\mathrm{Res}|\!|\!|_* = |\!|\!|a|\!|\!|. \tag{3.2}$$

The Helmholtz decomposition (3.1) shows for any $w \in u_D + V$ that

$$\varepsilon(w) - \mathbb{C}^{-1}\sigma_{\mathrm{AW}} = \varepsilon(w - u + a) + \mathbb{C}^{-1}\operatorname{Curl}\operatorname{Curl}\beta.$$

The aforementioned orthogonality reveals

$$\|\mathbb{C}^{-1}\sigma_{\mathrm{AW}} - \varepsilon(w)\|^2_{\mathbb{C}} = |\!|\!|w - u + a|\!|\!|^2 + \|\operatorname{Curl}\operatorname{Curl}\beta\|^2_{\mathbb{C}^{-1}}.$$

This is minimal for $w = u - a \in u_D + V$ and the minimum equals

$$\operatorname{dist}^2_{\mathbb{C}}(\mathbb{C}^{-1}\sigma_{\mathrm{AW}}, \varepsilon(u_D + V)) = \|\operatorname{Curl}\operatorname{Curl}\beta\|^2_{\mathbb{C}^{-1}}. \tag{3.3}$$

The combination of (3.1)–(3.3) concludes the proof. $\square$

3.2. **Reliability.** The data oscillations for the right-hand side f, with piecewise L^2 projection f_h onto $P_k(\mathcal{T};\mathbb{R}^2)$, and the Neumann boundary condition g, with piecewise L^2 projection g_h onto $P_k(\Gamma_N;\mathbb{R}^2)$ read

$$\operatorname{osc}(f,\mathcal{T})^2 := \sum_{T\in\mathcal{T}} h_T^2\|f-f_h\|_{L^2(T)}^2,$$
$$\operatorname{osc}(g,\mathcal{E}(\Gamma_N))^2 := \sum_{E\in\mathcal{E}(\Gamma_N)} h_E\|g-g_h\|_{L^2(E)}^2.$$

Let $j_{1,1}\le 3.83170597$ be the first positive root $j_{1,1}$ of the Bessel function of the first kind.

Lemma 3.3. *There exist constants $C_1, C_2, C_{korn} > 0$ such that*

$$|||\mathrm{Res}|||_* \le C_{korn}\operatorname{osc}(f,\mathcal{T})/j_{1,1} + C_1C_2(1+1/j_{1,1})C_{korn}\operatorname{osc}(g,\mathcal{E}(\Gamma_N)).$$

Proof. An integration by parts shows for any $v\in V$ that

$$\mathrm{Res}(v) = -\int_\Omega v\cdot\operatorname{div}(\sigma-\sigma_{\mathrm{AW}})\,dx + \int_{\Gamma_N} v\cdot(\sigma-\sigma_{\mathrm{AW}})\nu\,dx. \tag{3.4}$$

Let f_h be the piecewise L^2 projection onto $P_k(\mathcal{T};\mathbb{R}^2)$ and $v_T := \fint_T v\,dx \in \mathbb{R}^2$, then

$$-\int_\Omega v\cdot\operatorname{div}(\sigma-\sigma_{\mathrm{AW}})\,dx = \sum_{T\in\mathcal{T}}\int_T (v-v_T)\cdot(f-f_h)\,dx.$$

The Poincaré inequality [LS10], namely

$$\|v-v_T\|_{L^2(T)} \le h_T/j_{1,1}\|Dv\|_{L^2(T)},$$

for each triangle $T\in\mathcal{T}$, shows

$$-\int_\Omega v\cdot\operatorname{div}(\sigma-\sigma_{\mathrm{AW}})\,dx \le \|Dv\|\operatorname{osc}(f,\mathcal{T})/j_{1,1}.$$

The trace inequality shows for the piecewise L^2 projection $g_h=\sigma_{\mathrm{AW}}\nu$ onto $P_k(\Gamma_N;\mathbb{R}^2)$, and $v_E := \fint_{\omega_E} v\,dx$ with $E\in\mathcal{E}(T)\cap\mathcal{E}(\Gamma_N)$ and $T=\overline{\omega_E}\in\mathcal{T}$,

$$\begin{aligned}\int_{\Gamma_N} v\cdot(\sigma-\sigma_{\mathrm{AW}})\nu\,dx &= \sum_{E\in\mathcal{E}(\Gamma_N)}\int_E (v-v_E)\cdot(g-g_h)\,dx\\ &\le C_1\sum_{E\in\mathcal{E}(\Gamma_N)}\left(h_{\omega_E}^{-1/2}\|v-v_E\|_{L^2(\omega_E)} + h_{\omega_E}^{1/2}\|Dv\|_{L^2(\omega_E)}\right)\|g-g_h\|_{L^2(E)}\\ &\le C_1C_2(1+1/j_{1,1})\|Dv\|\operatorname{osc}(g,\mathcal{T}).\end{aligned}$$

The Korn inequality $\|Dv\|\le C_{korn}|||v|||$ concludes the proof. □

Lemma 3.4. *Given $\beta\in H^2(\Omega)$ with $\operatorname{Curl}\beta|_{\Gamma_j} = c_j\in\mathbb{R}^2$ for $j=0,\dots,J$, $\Gamma_N=\cup_{j=0}^J\Gamma_j$, there exists $\beta_A\in P_5(\mathcal{T})\cap H^2(\Omega)$ and some constant $C(\mathcal{T})>0$ such that*

$$\|h_{\mathcal{T}}^{-1}\operatorname{Curl}(\beta-\beta_A)\| + \|\operatorname{Curl}\operatorname{Curl}(\beta-\beta_A)\| \le C(\mathcal{T})\|\operatorname{Curl}\operatorname{Curl}\beta\|. \tag{3.5}$$

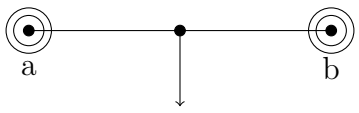

FIGURE 3.1. Edge degrees of freedom for the Argyris FEM

Proof. Given $\beta \in H^2(\Omega)$ with $\operatorname{Curl}\beta|_{\Gamma_j} = c_j \in \mathbb{R}^2$ for $j = 0, \ldots, J$, $\nu_E \cdot c_j = \partial\beta/\partial s$ for any $E \in \mathcal{E}(\Gamma_j)$ and hence β (resp. $\operatorname{Curl}\beta$) are piecewise affine (resp. constant) and continuous on Γ_j. Therefore, $\partial \operatorname{Curl}\beta/\partial s = 0$ along $E \in \mathcal{E}(\Gamma_j)$ may serve as values for the Argyris quasi interpolation, $\beta_{\rm A} = \beta$ in $\mathcal{N}(E) = \{a, b\}$, $D\beta_{\rm A} = D\beta$ in $\mathcal{N}(E)$ and $\operatorname{mid}(E)$, $\operatorname{Curl}\operatorname{Curl}(\beta - \beta_{\rm A})\nu_E = 0$ in $\mathcal{N}(E)$, c.f. Figure 3.1. Only the two degrees of freedom $\operatorname{Curl}\operatorname{Curl}\beta_{\rm A} \cdot \tau_E$ are left unpredicted at the endpoints a or b from the conditions on E but these may be determined by the condition $\operatorname{Curl}\operatorname{Curl}(\beta - \beta_{\rm A})\nu_E = 0$ on the neighbouring edges in Γ_j that may have different normal vectors. All remaining degrees of freedom are values of a patchwise polynomial L^2 approximation as in [Clé75]. This leads to (3.5) with a constant $C(\mathcal{T}) > 0$ that does only depend on the interior angles of the triangulation. □

The skew-symmetric functions γ in $L^2(\Omega; \mathbb{M}^{2\times 2}_{\rm skew})$ with $\operatorname{curl}_h \gamma$ belongs to $L^2(\Omega; \mathbb{R}^2)$ form the vector space $H(\operatorname{curl}, \mathcal{T}; \mathbb{M}^{2\times 2}_{\rm skew})$. Those functions have a trace in the tangential direction τ in the dual space $H^{-1/2}(\partial\Omega; \mathbb{R}^2)$ of the trace space $H^{1/2}(\partial\Omega; \mathbb{R}^2)$ written $\gamma\tau \in H^{-1/2}(\partial\Omega; \mathbb{R}^2)$. It is a technical extra smoothness assumption (which is met in all the numerical examples below) that $\gamma\tau \in L^2(\partial\Omega; \mathbb{R}^2)$ is a measurable function.

Lemma 3.5. *Any $\gamma \in H(\operatorname{curl}, \mathcal{T}; \mathbb{M}^{2\times 2}_{skew})$ with $\gamma\tau \in L^2(\Gamma_D; \mathbb{R}^2)$ satisfies*

$$\begin{aligned}\operatorname{dist}^2_{\mathbb{C}}(\mathbb{C}^{-1}\sigma_{AW}, \varepsilon(u_D + V)) \lesssim{}& \sum_{T\in\mathcal{T}} h_T^2 \|\operatorname{curl}(\mathbb{C}^{-1}\sigma_{AW} + \gamma)\|^2_{L^2(T)} \\ &+ \sum_{E\in\mathcal{E}(\Omega)} h_E \|[\mathbb{C}^{-1}\sigma_{AW} + \gamma]_E \tau_E\|^2_{L^2(E)} \\ &+ \sum_{E\in\mathcal{E}(\Gamma_D)} h_E \|(\mathbb{C}^{-1}\sigma_{AW} + \gamma - Du_D)\tau\|^2_{L^2(E)}.\end{aligned}$$

Proof. The decomposition (3.1) and the identity (3.3) prove that

$$\begin{aligned}\text{LHS} &:= \operatorname{dist}^2_{\mathbb{C}}(\mathbb{C}^{-1}\sigma_{\rm AW}, \varepsilon(u_D + V)) \\ &= \int_\Omega (\operatorname{Curl}\operatorname{Curl}\beta) : (\varepsilon(u - a) - \mathbb{C}^{-1}\sigma_{\rm AW})\, dx \\ &= \int_\Omega (\operatorname{Curl}\operatorname{Curl}\beta) : (\varepsilon(u) - \mathbb{C}^{-1}\sigma_{\rm AW})\, dx.\end{aligned}$$

Given β from Proposition 3.2, let β_A be defined as in Lemma 3.4. The point is that $\tau_{\rm AW} := \operatorname{Curl}\operatorname{Curl}\beta_{\rm A} \in \Sigma_{0,h}$ is an admissible divergence-free test function in the AW-MFEM because $\operatorname{div}\operatorname{Curl}\operatorname{Curl}\beta_A = 0$ a.e.

in Ω and $\partial \operatorname{Curl} \beta_A/\partial s = \partial \operatorname{Curl} \beta/\partial s = 0$ along any $E \in \mathcal{E}(\Gamma_N)$. Therefore (2.1)–(2.2) prove

$$\int_\Omega (\sigma - \sigma_{\mathrm{AW}}) : \mathbb{C}^{-1}\tau_{\mathrm{AW}}\, dx = 0.$$

Recall $\mathbb{C}^{-1}\sigma = \varepsilon(u)$ and reformulate this to prove

$$\int_\Omega \operatorname{Curl}\operatorname{Curl}(\beta_A) : (\varepsilon(u) - \mathbb{C}^{-1}\sigma_{AW})\, dx = 0. \tag{3.6}$$

The combination with the above identity of LHS plus the symmetry of $\operatorname{Curl}\operatorname{Curl}(\beta - \beta_A)$ show that

$$\mathrm{LHS} = \int_\Omega \operatorname{Curl}\operatorname{Curl}(\beta - \beta_A) : (D(u) - \mathbb{C}^{-1}\sigma_{\mathrm{AW}})\, dx.$$

An integration by parts provides the boundary term

$$\int_\Omega \operatorname{Curl}\operatorname{Curl}(\beta - \beta_{\mathrm{A}}) : D(u)\, dx = -\int_{\partial\Omega} \operatorname{Curl}(\beta - \beta_A) \cdot \frac{\partial u}{\partial s}\, ds$$

Since $\operatorname{Curl}(\beta) = c_j = \operatorname{Curl}(\beta_A)$ on Γ_j for any $j = 0, \ldots, J$ and since $u = u_D$ on Γ_D, it follows that

$$\int_\Omega \operatorname{Curl}\operatorname{Curl}(\beta - \beta_A) : D(u)\, dx = -\int_{\Gamma_D} \operatorname{Curl}(\beta - \beta_A) \cdot \frac{\partial u_D}{\partial s}\, ds. \tag{3.7}$$

On the other hand, any $\gamma \in H(\operatorname{curl}, \mathcal{T}; \mathbb{M}^{2\times 2}_{\mathrm{skew}})$ with $\gamma\tau \in L^2(\Gamma_D; \mathbb{R}^2)$ satisfies

$$\sum_{T\in\mathcal{T}} \int_T \operatorname{Curl}\operatorname{Curl}(\beta - \beta_A) : \gamma\, dx = 0.$$

Since $\operatorname{Curl}(\beta - \beta_A) = 0$ along Γ_N, an elementwise integration by parts shows

$$\begin{aligned}
&-\int_\Omega \operatorname{Curl}\operatorname{Curl}(\beta - \beta_A) : \mathbb{C}^{-1}\sigma_{\mathrm{AW}}\, dx \\
&\quad = -\sum_{T\in\mathcal{T}} \int_T \operatorname{Curl}(\beta - \beta_A) \cdot \operatorname{curl}(\mathbb{C}^{-1}\sigma_{\mathrm{AW}} + \gamma)\, dx \\
&\qquad + \sum_{E\in\mathcal{E}(\Omega)} \int_E \operatorname{Curl}(\beta - \beta_A) \cdot ([\mathbb{C}^{-1}\sigma_{\mathrm{AW}} + \gamma]_E \tau_E)\, ds \\
&\qquad + \sum_{E\in\Gamma_D} \int_E \operatorname{Curl}(\beta - \beta_A) \cdot ((\mathbb{C}^{-1}\sigma_{\mathrm{AW}} + \gamma)\tau)\, ds.
\end{aligned} \tag{3.8}$$

The combination of the previous identities (3.6)–(3.8) reads

$$\begin{aligned}\mathrm{LHS} &\le \sum_{T\in\mathcal{T}} h_T\|\mathrm{curl}(\mathbb{C}^{-1}\sigma_{\mathrm{AW}}+\gamma)\|_{L^2(T)}h_T^{-1}\|\mathrm{Curl}(\beta-\beta_A)\|_{L^2(T)}\\ &+\sum_{E\in\mathcal{E}(\Omega)} h_E^{1/2}\|[\mathbb{C}^{-1}\sigma_{\mathrm{AW}}+\gamma]_E\tau_E\|_{L^2(E)}h_E^{-1/2}\|\mathrm{Curl}(\beta-\beta_A)\|_{L^2(E)}\\ &+\sum_{E\in\mathcal{E}(\Gamma_D)} h_E^{1/2}\|(\mathbb{C}^{-1}\sigma_{\mathrm{AW}}+\gamma-Du_D)\tau\|_{L^2(E)}h_E^{-1/2}\|\mathrm{Curl}(\beta-\beta_A)\|_{L^2(E)}.\end{aligned}$$

The Cauchy-Schwarz inequality, the error estimate (3.5), plus

$$\mathrm{LHS}^{1/2}=\mathrm{dist}_{\mathbb{C}}(\mathbb{C}^{-1}\sigma_{\mathrm{AW}},\varepsilon(u_D+V))=\|\mathrm{Curl}\,\mathrm{Curl}\,\beta\|_{\mathbb{C}^{-1}}$$

conclude the proof. □

The subsequent theorem summarises all the terms as indicated in (1.2) of the introduction.

Theorem 3.6. *Any $\gamma\in H(\mathrm{curl},\mathcal{T};\mathbb{M}^{2\times2}_{skew})$ with $\gamma\tau\in L^2(\Gamma_D;\mathbb{R}^2)$ satisfies*

$$\begin{aligned}\|\sigma-\sigma_{AW}\|^2_{\mathbb{C}^{-1}} &\lesssim \mathrm{osc}^2(f,\mathcal{T})+\mathrm{osc}^2(g,\mathcal{E}(\Gamma_N))\\ &+\sum_{T\in\mathcal{T}} h_T^2\|\mathrm{curl}(\mathbb{C}^{-1}\sigma_{AW}+\gamma)\|^2_{L^2(T)}\\ &+\sum_{E\in\mathcal{E}(\Omega)} h_E\|[\mathbb{C}^{-1}\sigma_{AW}+\gamma]_E\tau_E\|^2_{L^2(E)}\\ &+\sum_{E\in\mathcal{E}(\Gamma_D)} h_E\|(\mathbb{C}^{-1}\sigma_{AW}+\gamma-Du_D)\tau\|^2_{L^2(E)}.\end{aligned}$$

Proof. The result follows from the combination of the previous Theorem 3.1, Lemmas 3.3 and 3.5. □

The a posteriori estimate of Theorem 3.6 holds for any $\gamma\in H^1(\mathcal{T};\mathbb{M}^{2\times2}_{\mathrm{skew}})$. The particular choice of the polynomial approximation γ_h of γ enters the efficiency estimate in Lemmas 3.7–3.8 and therefore should be a sufficiently accurate approximation of $\mathrm{skew}(Du)$. Hence, one might solve the displacement formulation with high polynomial degree or even minimise the a posteriori error estimator with respect to γ_h. Since this does involve high computational costs, a cheap local post-processing is introduced in the next section.

3.3. **Efficiency.** Any practical choice of γ in the a posteriori error bounds of Theorem 3.6 involves some polynomial approximation $\gamma_h\in P_k(\mathcal{T};\,\mathbb{M}^{2\times2}_{\mathrm{skew}})$ of γ. Then the inverse estimate technique from [Ver96] guarantees local efficiency in the sense that all the volume and edge contributions are bounded in terms of the local error plus the error term $\|\mathrm{skew}(Du)-\gamma_h\|$ as shown in the three lemmas of this subsection, which imply (1.3) of the introduction.

The analysis involves an extension operator $L : C^0(E) \to C^0(T)$, $E \in \mathcal{E}(T)$, $T \in \mathcal{T}$, that extends polynomials of degree $\leq k$ on E to polynomials of the same degree on T and satisfies $(Lp)|_E = p|_E$ [Ver94, (4.1)–(4.2)]. Let $b_T := 27\,\lambda_1\lambda_2\lambda_3$ denote the volume-bubble function and $b_E := 4\,\lambda_a\lambda_b$ the edge-bubble function for the three barycentric coordinates $\lambda_1, \lambda_2, \lambda_3$ of the triangle T with an edge E of vertices a and b. Any $v \in P_k(T)$ with $v \in P_k(E)$ satisfies [Ver94, Lemma 4.1]

$$
\begin{aligned}
\|b_T v\|_{L^2(T)} &\lesssim \|v\|_{L^2(T)} \lesssim \|b_T^{1/2} v\|_{L^2(T)},\\
\|b_E v\|_{L^2(E)} &\lesssim \|v\|_{L^2(E)} \lesssim \|b_E^{1/2} v\|_{L^2(E)},\\
h_E^{1/2}\|v\|_{L^2(E)} &\lesssim \|b_E^{1/2} Lv\|_{L^2(T)} \lesssim h_E^{1/2}\|v\|_{L^2(E)}.
\end{aligned}
\tag{3.9}
$$

Lemma 3.7. *Any $T \in \mathcal{T}$ satisfies*

$$
\begin{aligned}
h_T\|\mathrm{curl}(\mathbb{C}^{-1}\sigma_{AW} + \gamma_h)\|_{L^2(T)} \lesssim \|\mathbb{C}^{-1}(\sigma - \sigma_{AW})\|_{L^2(T)}\\
+ \|skew(Du) - \gamma_h\|_{L^2(T)}.
\end{aligned}
$$

Proof. An integration by parts together with (3.9) yields

$$
\begin{aligned}
&\|\mathrm{curl}(\mathbb{C}^{-1}\sigma_{\mathrm{AW}} + \gamma_h)\|_{L^2(T)}^2\\
&\quad\lesssim \|b_T^{1/2}\,\mathrm{curl}(\mathbb{C}^{-1}\sigma_{\mathrm{AW}} + \gamma_h)\|_{L^2(T)}^2\\
&\quad= -\int_T b_T\left(\mathrm{curl}(Du - \mathbb{C}^{-1}\sigma_{\mathrm{AW}} - \gamma_h)\cdot\mathrm{curl}(\mathbb{C}^{-1}\sigma_{\mathrm{AW}} + \gamma_h)\right)\,dx\\
&\quad= \int_T (Du - \mathbb{C}^{-1}\sigma_{\mathrm{AW}} - \gamma_h) : \mathrm{Curl}(b_T\,\mathrm{curl}(\mathbb{C}^{-1}\sigma_{\mathrm{AW}} + \gamma_h))\,dx\\
&\quad\leq \|Du - \mathbb{C}^{-1}\sigma_{\mathrm{AW}} - \gamma_h\|_{L^2(T)}\|\mathrm{Curl}(b_T\,\mathrm{curl}(\mathbb{C}^{-1}\sigma_{\mathrm{AW}} + \gamma_h))\|_{L^2(T)}.
\end{aligned}
$$

A discrete inverse inequality plus (3.9) leads to

$$
\begin{aligned}
\|\mathrm{Curl}(b_T\,\mathrm{curl}(\mathbb{C}^{-1}\sigma_{\mathrm{AW}} + \gamma_h))\|_{L^2(T)} &\lesssim h_T^{-1}\|b_T\,\mathrm{curl}(\mathbb{C}^{-1}\sigma_{\mathrm{AW}} + \gamma_h)\|_{L^2(T)}\\
&\lesssim h_T^{-1}\|\mathrm{curl}(\mathbb{C}^{-1}\sigma_{\mathrm{AW}} + \gamma_h)\|_{L^2(T)}.
\end{aligned}
$$

The previous two estimates and the triangle inequality conclude the proof. □

Lemma 3.8. *Any $E \in \mathcal{E}(\Omega)$ satisfies*

$$
\begin{aligned}
h_E^{1/2}\|[\mathbb{C}^{-1}\sigma_{AW} + \gamma_h]\tau_E\|_{L^2(E)} \lesssim \|\mathbb{C}^{-1}(\sigma - \sigma_{AW})\|_{L^2(\omega_E)}\\
+ \|skew(Du) - \gamma_h\|_{L^2(\omega_E)}.
\end{aligned}
$$

Proof. Given $v_h = [\mathbb{C}^{-1}\sigma_{\mathrm{AW}} + \gamma_h]\tau_E$, (3.9) reads

$$
\|v_h\|_{L^2(E)}^2 \lesssim \|b_E^{1/2} v_h\|_{L^2(E)}^2 = \int_E v_h b_E Lv_h\,ds.
\tag{3.10}
$$

An integration by parts with $Du = \mathbb{C}^{-1}\sigma + \mathrm{skew}(Du)$ and the piecewise curl operator curl_h shows

$$\begin{aligned}\int_E v_h \cdot b_E L v_h \, ds &= \int_{\omega_E} \mathrm{curl}_h(\mathbb{C}^{-1}\sigma_{\mathrm{AW}} + \gamma_h) \cdot (b_E L v_h)\, dx \\ &\quad + \int_{\omega_E} (Du - \mathbb{C}^{-1}\sigma_{\mathrm{AW}} - \gamma_h) : \mathrm{Curl}(b_E L v_h)\, dx.\end{aligned} \tag{3.11}$$

Hence, (3.10)–(3.11) lead to

$$\begin{aligned}\|v_h\|^2_{L^2(E)} &\lesssim \|\mathrm{curl}_h(\mathbb{C}^{-1}\sigma_{\mathrm{AW}} + \gamma_h)\|_{L^2(\omega_E)} \|b_E L v_h\|_{L^2(\omega_E)} \\ &\quad + \|Du - \mathbb{C}^{-1}\sigma_{\mathrm{AW}} - \gamma_h\|_{L^2(\omega_E)} \|\mathrm{Curl}(b_E L v_h)\|_{L^2(\omega_E)}.\end{aligned}$$

The proof of Lemma 3.7 shows

$$\|\mathrm{curl}_h(\mathbb{C}^{-1}\sigma_{\mathrm{AW}} + \gamma_h)\|_{L^2(\omega_E)} \lesssim h_E^{-1} \|Du - \mathbb{C}^{-1}\sigma_{\mathrm{AW}} - \gamma_h\|_{L^2(\omega_E)}.$$

Together with the discrete inverse estimate

$$\|\mathrm{Curl}(b_E L v_h)\|_{L^2(\omega_E)} \lesssim h_E^{-1} \|b_E L v_h\|_{L^2(\omega_E)}$$

plus (3.9), this yields

$$h_E^{1/2} \|v_h\|_{L^2(E)} \lesssim \|Du - \mathbb{C}^{-1}\sigma_{\mathrm{AW}} - \gamma_h\|_{L^2(\omega_E)}.$$

The triangle inequality concludes the proof. □

Lemma 3.9. *Any $E \in \mathcal{E}(\Gamma_D)$ satisfies*

$$\begin{aligned}h_E^{1/2} \|(\mathbb{C}^{-1}\sigma_{AW} + \gamma_h - Du_D)\tau\|_{L^2(E)} &\lesssim \|\mathbb{C}^{-1}(\sigma - \sigma_{AW})\|_{L^2(\omega_E)} \\ &\quad + \|skew(Du) - \gamma_h\|_{L^2(\omega_E)}.\end{aligned}$$

Proof. Set $\overline{\omega_E} = T \in \mathcal{T}$ and $v_h := (\mathbb{C}^{-1}\sigma_{\mathrm{AW}} + \gamma_h - Du_D)\tau$. Then (3.9) and an integration by parts lead to

$$\begin{aligned}\|v_h\|^2_{L^2(E)} \lesssim \int_E v_h \cdot b_E L v_h \, ds &= \int_{\omega_E} \mathrm{curl}(\mathbb{C}^{-1}\sigma_{\mathrm{AW}} + \gamma_h) \cdot (b_E L v_h)\, dx \\ &\quad + \int_{\omega_E} (Du - \mathbb{C}^{-1}\sigma_{\mathrm{AW}} - \gamma_h) : \mathrm{Curl}(b_E L v_h)\, dx.\end{aligned}$$

The arguments of the proof of Lemma 3.8 conclude the proof. □

4. Post-processing

Since σ_h approximates $\mathbb{C}\varepsilon(u)$, an improved approximate solution of the displacement u follows from local post-processing in the spirit of Stenberg [Ste88]. Let

$$\begin{aligned}\mathcal{RM}(\mathcal{T}) := \{v \in L^2(\mathcal{T};\mathbb{R}^2) \,|\, v &= c + b(x_2, -x_1)^t, \\ &c \in \mathbb{R}^2, b \in \mathbb{R}, \text{ for all } T \in \mathcal{T}\}\end{aligned}$$

denote the space of rigid body motions. For $m \geq k+2$ define $u_h^* \in P_m(\mathcal{T};\mathbb{R}^2)$ on each $T \in \mathcal{T}$ with the (local) L^2 projection Π_T onto $\mathcal{RM}(T)$ under the side condition $\Pi_T u_h^* = \Pi_T u_h$ as the solution to

$$\int_T \mathbb{C}\varepsilon(u_h^*) : \varepsilon(v)\,dx = \int_T \sigma_h : \varepsilon(v)\,dx \quad \forall v \in (\mathrm{id}-\Pi_T)P_m(T;\mathbb{R}^2). \tag{4.1}$$

In other words, $u_h^*|_T \in P_m(T;\mathbb{R}^2)$ is the Riesz representation of the linear functional $\int_T \sigma_h : \varepsilon(\cdot)\,dx$ in the Hilbert space

$$(\mathrm{id}-\Pi_T)P_m(\mathcal{T};\mathbb{R}^2) \equiv \{v_m \in P_m(T;\mathbb{R}^2) \mid \int_T v_m \cdot w_k dx = 0 \text{ for all } w_k \in \mathcal{RM}(T)\}.$$

The post-processing on each triangle with Lagrange-multiplier $\lambda_{rm} \in \mathcal{RM}(T)$ can be implemented as the linear system of equations

$$\int_T \varepsilon(u_h^*) : \varepsilon(v_m)\,dx + \int_T \lambda_{rm} \cdot v_m = \int_T \mathbb{C}^{-1}\sigma_h : \varepsilon(v_m)\,dx \quad \text{for all } v_m \in P_m(T;\mathbb{R}^2),$$

$$\int_T u_h^* \cdot w_{rm}\,dx = \int_T u_h \cdot w_{rm}\,dx \text{ for all } w_{rm} \in \mathcal{RM}(T).$$

Since $\mathcal{RM}(T) \subset P_m(T;\mathbb{R}^2)$, the first Korn inequality [Bra01] shows for any $\lambda_{rm} \in \mathcal{RM}(T)$, with $\varepsilon(\lambda_{rm}) = 0$,

$$\begin{aligned}\|\lambda_{rm}\|_{L^2(T)} &= \frac{\int_T \lambda_{rm}^2\,dx}{\|\lambda_{rm}\|_{L^2(T)} + \|\varepsilon(\lambda_{rm})\|_{L^2(T)}} \\ &\leq \sup_{\substack{v_m \in P_m(T;\mathbb{R}^2) \\ v_m \not\equiv 0}} \frac{\int_T \lambda_{rm} v_m\,dx}{\|v_m\|_{L^2(T)} + \|\varepsilon(v_m)\|_{L^2(T)}} \\ &\leq C_{korn}^{-1} \sup_{\substack{v_m \in P_m(T;\mathbb{R}^2) \\ v_m \not\equiv 0}} \frac{\int_T \lambda_{rm} v_m\,dx}{\|v_m\|_{H^1(T)}}.\end{aligned}$$

Thus, the Brezzi splitting theorem [Bre74] shows that there exists a unique solution $u_h^*|_T$ on each triangle $T \in \mathcal{T}$ that lead to the globally discontinuous solution $u_h^* \in P_m(\mathcal{T};\mathbb{R}^2)$.

The following theorem serves as a motivation for the choice of $\gamma_h := \mathrm{skew}(Du_h^*) \in H^1(\mathcal{T};\mathbb{M}^{2\times 2}_{\mathrm{skew}})$ in the numerical examples. For sufficiently smooth boundary and smooth data f, $g = 0$, and $u_D = 0$, the following regularity

$$\|u\|_{H^2(\Omega)} + \|\sigma\|_{H^1(\Omega)} \leq C\|f\|_{L^2(\Omega)}, \tag{4.2}$$

is known with a constant $C > 0$ that is independent of the Poisson ratio $\nu \to 1/2$ [Vog83, Theorem A.1]. It appears as a gap of the theory to pose the regularity assumption (4.2) (having a smooth boundary $\partial\Omega$ in mind) and assume triangles (matching a polygonal boundary $\partial\Omega$ exactly). However, this is not the place to discuss curved triangles

and the boundary approximation for practical examples face points on the boundary, where the type of the boundary condition changes or other inconsistent boundary conditions enforce singular solutions and require adaptive mesh-refining. Nevertheless, the subsequent theorem indicates that the post-processing leads to a better approximation in a smooth situation at least. It will be the outcome of the numerical experiments to justify indirectly this form of a post-processing.

Theorem 4.1. *Suppose the regularity assumption* (4.2) *and that* $u \in H^{m+1}(\Omega)$, $\sigma \in H^{k+2}(\Omega;\mathbb{S})$, *and* $f = \operatorname{div}\sigma \in H^{k+1}(\Omega)$. *Then the post-processed displacement* $u_h^* \in P_m(\mathcal{T};\mathbb{R}^2)$ *and the corresponding post-processed stress* $\sigma_h^* := \mathbb{C}\varepsilon_h(u_h^*) \in P_{m-1}(\mathcal{T};\mathbb{S})$ *satisfy*

$$\|u-u_h^*\|_{L^2(\Omega)} \lesssim h^{k+3}(\|\sigma\|_{H^{k+2}(\Omega)} + \|\operatorname{div}\sigma\|_{H^{k+1}(\Omega)}) + h^{m+1}\|u\|_{H^{m+1}(\Omega)},$$
$$\|\sigma-\sigma_h^*\|_{L^2(\Omega)} \lesssim Ch^{k+2}\|\sigma\|_{H^{k+2}(\Omega)} + h^m\|u\|_{H^{m+1}(\Omega)}.$$

Recall that the generic constant C hidden in the notation $\lesssim$ only depends on the Lamè parameter μ and neither on the critical Lamè parameter λ nor the maximal mesh-size h in the shape-regular triangulation $\mathcal{T}$.

The proof is based on the following lemma where P_h is the L^2 projection onto V_h with the well-known approximation property

$$\|P_hv - v\|_{L^2(\Omega)} \lesssim h^{k+1}\|v\|_{H^{k+1}(\Omega)} \quad \text{for all } v \in H^{k+1}(\Omega). \tag{4.3}$$

Lemma 4.2. *With sufficiently smooth boundary* $\partial\Omega$, $\sigma \in H^{k+2}(\Omega;\mathbb{S})$ *and* $f = \operatorname{div}\sigma \in H^{k+1}(\Omega)$, *it holds that*

$$\|P_hu - u_h\|_{L^2(\Omega)} \lesssim h^{k+3}\left(\|\sigma\|_{H^{k+2}(\Omega)} + \|\operatorname{div}\sigma\|_{H^{k+1}(\Omega)}\right). \tag{4.4}$$

Proof. Let $(\eta, z) \in \Sigma_0 \times L^2(\Omega;\mathbb{R}^2)$ be the dual solution to

$$\begin{aligned} \int_\Omega \eta : \mathbb{C}^{-1}\tau\,dx + \int_\Omega z\cdot\operatorname{div}\tau\,dx = 0 \quad &\text{for all } \tau \in \Sigma_0, \\ \int_\Omega v\cdot\operatorname{div}\eta\,dx = \int_\Omega (P_hu-u_h)\cdot v\,dx \quad &\text{for all } v \in V. \end{aligned} \tag{4.5}$$

Let Π_{AW} denote the projection onto $AW_k(\mathcal{T})$ that satisfies $\operatorname{div}\Pi_{\mathrm{AW}} = P_h\operatorname{div}$ [AW02], then (4.5) leads to

$$\|P_hu-u_h\|_{L^2(\Omega)}^2 = \int_\Omega (P_hu-u_h)\cdot\operatorname{div}\eta\,dx \tag{4.6}$$

$$= \int_\Omega (P_hu-u_h)\cdot P_h\operatorname{div}\eta\,dx = \int_\Omega (u-u_h)\cdot\operatorname{div}\Pi_{\mathrm{AW}}\eta\,dx. \tag{4.7}$$

The difference of (2.1) and (2.2) reads

$$\begin{aligned} \int_\Omega (\sigma-\sigma_h) : \mathbb{C}^{-1}\tau_h\,dx + \int_\Omega (u-u_h)\operatorname{div}\tau_h = 0 \quad &\text{for all } \tau_h \in \Sigma_{0,h}, \\ \int_\Omega v_h\cdot\operatorname{div}(\sigma-\sigma_h)\,dx = 0 \quad &\text{for all } v_h \in V_h. \end{aligned}$$

This, (4.5) and (4.6) lead to

$$\begin{aligned}
&\|P_h u - u_h\|_{L^2(\Omega)}^2 \\
&= -\int_\Omega (\sigma - \sigma_h) : \mathbb{C}^{-1}(\Pi_{\mathrm{AW}}\eta - \eta)\,dx - \int_\Omega (\sigma - \sigma_h) : \mathbb{C}^{-1}\eta\,dx \\
&= -\int_\Omega (\sigma - \sigma_h) : \mathbb{C}^{-1}(\Pi_{\mathrm{AW}}\eta - \eta)\,dx + \int_\Omega (z - P_h z)\cdot \mathrm{div}(\sigma - \sigma_h)\,dx \\
&\lesssim h\|\sigma - \sigma_h\|_{L^2(\Omega)}\|\eta\|_{H^1(\Omega)} + h^2\|\mathrm{div}(\sigma - \sigma_h)\|_{L^2(\Omega)}\|z\|_{H^2(\Omega)}.
\end{aligned}$$

The a priori estimate (4.2) implies

$$\|z\|_{H^2(\Omega)} \lesssim \|P_h u - u_h\|_{L^2(\Omega)} \quad \text{and} \quad \|\eta\|_{H^1(\Omega)} \lesssim \|P_h u - u_h\|_{L^2(\Omega)}.$$

This together with Theorem 2.1 yields

$$\|P_h u - u_h\|_{L^2(\Omega)} \lesssim h^{k+3}\left(\|\sigma\|_{H^{k+2}(\Omega)} + \|\mathrm{div}\,\sigma\|_{H^{k+1}(\Omega)}\right). \qquad \square$$

Proof of Theorem 4.1. Let $\hat{u}$ be the L^2 projection of u onto $P_m(\mathcal{T};\mathbb{R}^2)$ and Π_h denote the L^2 projection onto $\mathcal{RM}$. The triangle inequality shows

$$\begin{aligned}
\|u - u_h^*\|_{L^2(\Omega)} \le{}& \|u - \hat{u}\|_{L^2(\Omega)} + \|\Pi_h(\hat{u} - u_h^*)\|_{L^2(\Omega)} \\
&+ \|(\mathrm{id} - \Pi_h)(\hat{u} - u_h^*)\|_{L^2(\Omega)}.
\end{aligned} \tag{4.8}$$

Since $\hat{u}$ is the L^2-projection of u onto $P_m(\mathcal{T};\mathbb{R}^2)$, the a priori estimate (4.3) shows for the first term on the right-hand side of (4.8) that

$$\|u - \hat{u}\|_{L^2(\Omega)} \lesssim h^{m+1}\|u\|_{H^{m+1}(\Omega)} \quad \text{for all } u \in H^{m+1}(\Omega). \tag{4.9}$$

For the second term of (4.8), notice that $\Pi_T u_h^* = \Pi_T u_h$ on each T implies $\|\Pi_T(\hat{u} - u_h^*)\|_{L^2(T)} = \|\Pi_T\hat{u} - \Pi_T u_h\|_{L^2(T)}$. This and the boundedness of Π_T show

$$\|\Pi_T(\hat{u} - u_h^*)\|_{L^2(T)} \lesssim \|u - \hat{u}\|_{L^2(T)} + \|\Pi_T(u - u_h)\|_{L^2(T)}.$$

The first term is estimated in (4.9), since $\Pi_T P_h|_T = \Pi_T$, the second term yields

$$\|\Pi_T(u - u_h)\|_{L^2(T)} = \|\Pi_T(P_h u - u_h)\|_{L^2(T)} \lesssim \|P_h u - u_h\|_{L^2(T)}.$$

Lemma 4.2 shows

$$\|P_h u - u_h\|_{L^2(\Omega)} \lesssim h^{k+3}\left(\|\sigma\|_{H^{k+2}(\Omega)} + \|\mathrm{div}\,\sigma\|_{H^{k+1}(\Omega)}\right). \tag{4.10}$$

In order to bound the third term on the right-hand side of (4.8), consider the perturbed saddle point problem to (4.1). With $\mathbb{C}\varepsilon = 2\mu\varepsilon + \lambda\,\mathrm{id}\,\mathrm{tr}(\varepsilon)$, it reads

$$\begin{aligned}
2\mu\int_T \varepsilon(u_h^*) : \varepsilon(v)\,dx + \int_T p_h^*\,\mathrm{div}\,v\,dx &= \int_T \sigma_h : \varepsilon(v)\,dx \\
&\text{for all } v \in (\mathrm{id} - \Pi_T)P_m(T;\mathbb{R}^2), \\
-\frac{1}{\lambda}\int_T p_h^* q\,dx + \int_T q\,\mathrm{div}u_h^*\,dx &= 0 \quad \text{for all } q \in P_{m-1}(T;\mathbb{R}).
\end{aligned} \tag{4.11}$$

The solution of (4.1) satisfies (4.11) with $p_h^* = \lambda \operatorname{div} u_h^*$. The stability of the unperturbed saddle point problem (with $\lambda = \infty$), namely

$$\|q\|_{L^2(T)} \lesssim \sup_{0\neq v\in(\mathrm{id}-\Pi_T)P_m(T;\mathbb{R}^2)} \frac{\int_T q \operatorname{div} v\, dx}{\|\varepsilon(v)\|_{L^2(T)}} \quad \text{for all } q \in P_{m-1}(T;\mathbb{R}),$$

implies uniform stability of the perturbed problem with respect to λ [Bra01]. Hence, there exist $v \in (\mathrm{id}-\Pi_T)P_m(T;\mathbb{R}^2)$ and $q \in P_{m-1}(T;\mathbb{R})$ such that the L^2 projections $\hat{u} \in (\mathrm{id} - \Pi_T)P_m(T;\mathbb{R}^2)$ of u and $\hat{p} \in P_{m-1}(T;\mathbb{R})$ of p satisfy

$$\begin{aligned}\|\varepsilon(u_h^* - \hat{u})\|_{L^2(T)} + \|p_h^* - \hat{p}\|_{L^2(T)} &\le 2\mu \int_T \varepsilon(u_h^* - \hat{u}) : \varepsilon(v)\, dx \\ + \int_T (p_h^* - \hat{p}) \operatorname{div} v\, dx - \frac{1}{\lambda}\int_T (p_h^* - \hat{p}) q\, dx &+ \int_T q \operatorname{div}(u_h^* - \hat{u})\, dx\end{aligned}$$

and there exists a constant $C > 0$ independent on λ such that

$$\|\varepsilon(v)\|_{L^2(T)} + \|q\|_{L^2(T)} \le C. \tag{4.12}$$

Let $p = \lambda \operatorname{div} u$, then (4.11) and $\operatorname{div} v \in P_{m-1}(T;\mathbb{R})$ yield

$$\begin{aligned}&\|\varepsilon(u_h^* - \hat{u})\|_{L^2(T)} + \|p_h^* - \hat{p}\|_{L^2(T)} \\ &\le 2\mu \int_T \varepsilon(u - \hat{u}) : \varepsilon(v)\, dx + \int_T (p - \hat{p}) \operatorname{div} v\, dx - \frac{1}{\lambda}\int_T (p - \hat{p}) q\, dx \\ &\quad + \int_T q \operatorname{div}(u - \hat{u})\, dx - \int_T (\sigma - \sigma_h) : \varepsilon(v)\, dx \\ &\le 2\mu \|u - \hat{u}\|_{H^1(T)} \|\varepsilon(v)\|_{L^2(T)} + \|u - \hat{u}\|_{H^1(T)} \|q\|_{L^2(T)} \\ &\quad + \|\sigma - \sigma_h\|_{L^2(T)} \|\varepsilon(v)\|_{L^2(T)}.\end{aligned}$$

This and (4.12) show for some C that does depend on μ but not on λ,

$$\begin{aligned}&\|\varepsilon(u_h^* - \hat{u})\|_{L^2(T)} + \|p_h^* - \hat{p}\|_{L^2(T)} \\ &\qquad \le C\left(\|u - \hat{u}\|_{H^1(T)} + \|\sigma - \sigma_h\|_{L^2(T)}\right).\end{aligned} \tag{4.13}$$

Define $v \in P_m(T;\mathbb{R}^2)$ by $v = (\mathrm{id} - \Pi_T)(\hat{u} - u_h^*)$. Since $v \perp \mathcal{RM}(T)$, the second Korn inequality [Bra01] leads to

$$\|v\|_{L^2(T)} \lesssim h_T \|\varepsilon(v)\|_{L^2(T)}.$$

Since $\varepsilon(\Pi_T(\hat{u} - u_h^*)) = 0$, this and (4.13) show

$$\|(\mathrm{id} - \Pi_T)(\hat{u} - u_h^*)\|_{L^2(T)} \lesssim h_T \|u - \hat{u}\|_{H^1(T)} + h_T \|\sigma - \sigma_h\|_{L^2(T)}.$$

Let I_h denote the nodal interpolant $I_h|_T : H^{m+1}(T) \to P_m(T;\mathbb{R}^2)$ with the interpolation estimate [BS94]

$$|u - I_h u|_{H^\mu(T)} \lesssim h_T^{m+1-\mu} |u|_{H^{m+1}(T)} \quad \forall u \in H^{m+1}(T),\ \mu = 0, 1. \tag{4.14}$$

The triangle inequality and an inverse estimate show

$$\begin{aligned}|u-\hat{u}|_{H^1(T)} &\leq |u-I_hu|_{H^1(T)}+|I_hu-\hat{u}|_{H^1(T)}\\ &\lesssim |u-I_hu|_{H^1(T)}+h_T^{-1}\|I_hu-\hat{u}\|_{L^2(T)}\\ &\leq |u-I_hu|_{H^1(T)}+h_T^{-1}\|u-I_hu\|_{L^2(T)}+h_T^{-1}\|u-\hat{u}\|_{L^2(T)}.\end{aligned}$$

The interpolation estimates (4.14) and the approximation property (4.3) yield

$$\|u-\hat{u}\|_{H^1(\Omega)}\lesssim h^m\|u\|_{H^{m+1}(\Omega)}.$$

This and Theorem 2.1 lead to the estimate for the third term of (4.8)

$$\|(\mathrm{id}-\Pi_T)(\hat{u}-u_h^*)\|_{L^2(\Omega)}\lesssim h^{m+1}\|u\|_{H^{m+1}(\Omega)}+h^{k+3}\|\sigma\|_{H^{k+2}(\Omega)}.$$

For the second assertion a triangle inequality for the L^2 projection $\hat{\sigma}\in P_{m-1}(T;\mathbb{S})$ of σ shows

$$\|\sigma-\sigma_h^*\|_{L^2(\Omega)}\leq\|\sigma-\hat{\sigma}\|_{L^2(\Omega)}+\|\sigma_h^*-\hat{\sigma}\|_{L^2(\Omega)}.$$

Since

$$\|\sigma_h^*-\hat{\sigma}\|_{L^2(\Omega)}\leq\|\varepsilon(u_h^*-\hat{u})\|_{L^2(T)}+\|p_h^*-\hat{p}\|_{L^2(T)},$$

the estimates for (4.13) and the L^2 projection estimate

$$\|\sigma-\hat{\sigma}\|_{L^2(\Omega)}\lesssim h^{k+2}\|\sigma\|_{H^{k+2}(\Omega)},$$

show that

$$\|\sigma-\sigma_h^*\|_{L^2(\Omega)}\lesssim h^{k+2}\|\sigma\|_{H^{k+2}(\Omega)}+h^m\|u\|_{H^{m+1}(\Omega)}.\qquad\square$$

5. Numerical experiments

This section is devoted to four numerical benchmarks. The experiments verify reliability and efficiency of the proposed residual-based a posteriori error estimator for uniform and adaptive mesh-refinements.

5.1. **The adaptive finite element method.** The adaptive finite element method computes sequences of discrete subspaces $(\Sigma_{g,\ell})_\ell$ and $(V_\ell)_\ell$ throughout successive local refinement of the domain Ω. The corresponding sequence of meshes $(\mathcal{T}_\ell)_\ell$ consists of nested regular triangulations. The AFEM consists of the following loop

$$\text{Solve}\to\text{Estimate}\to\text{Mark}\to\text{Refine}.$$

Solve. Given a mesh $\mathcal{T}_\ell$ the step Solve calculates the solution of the finite-dimensional saddle point problem

$$\begin{pmatrix}A & B^t\\ B & \end{pmatrix}\begin{pmatrix}x\\ y\end{pmatrix}=\begin{pmatrix}b_D\\ b_f\end{pmatrix}.$$

The system matrices A and B, and the right-hand sides b_D and b_g are computed for the basis $\operatorname{span}\{\tau_j\} = \Sigma_{g,\ell}$ and $\operatorname{span}\{v_j\} = V_\ell$ by

$$A_{jk} := \int_\Omega \tau_j : \mathbb{C}^{-1}\tau_k \, dx \quad \text{and} \quad B_{jk} := \int_\Omega v_j \cdot \operatorname{div} \sigma_k \, dx;$$
$$b_{D,j} := \int_{\Gamma_D} u_D \cdot (\tau_j \nu) \, ds \quad \text{and} \quad b_{f,j} := \int_\Omega f \cdot v_j \, dx.$$

The discrete solutions for the stress tensor σ_ℓ and the displacement u_ℓ are given by

$$\sigma_\ell = \sum_{k=1}^{\dim(\Sigma_{g,\ell})} x_k \tau_k \quad \text{and} \quad u_\ell = \sum_{k=1}^{\dim(V_\ell)} y_k v_k.$$

For more details on the assembly of these matrices cf. [CGRT08, CEG11]. In contrast to [CGRT08], for adaptive computations the basis functions τ_k need to be scaled in order to improve the condition number. Nodal degrees of freedom are weighted with $\omega_z^{-1/2}$, edge degrees of freedom with $\omega_E^{-1/2}$ and element degrees of freedom with $|T|^{-1/2}$, where ω_z and ω_E denote the nodal and edge patches. This improvement over [CGRT08] allows more stable calculations and appears to be significant.

Estimate. The error $\|\sigma - \sigma_{\mathrm{AW}}\|^2_{\mathbb{C}^{-1}}$ is estimated a posteriori by

$$\begin{aligned}\eta_\ell^2 &= \operatorname{osc}^2(f, \mathcal{T}) + \operatorname{osc}^2(g, \mathcal{E}(\Gamma_N)) \\ &\quad + \sum_{T\in\mathcal{T}} h_T^2 \|\operatorname{curl}(\mathbb{C}^{-1}\sigma_\ell + \operatorname{skew}(Du_\ell^*))\|^2_{L^2(T)} \\ &\quad + \sum_{E\in\mathcal{E}(\Omega)} h_E \|[\mathbb{C}^{-1}\sigma_\ell + \operatorname{skew}(Du_\ell^*)]_E \tau_E\|^2_{L^2(E)} \\ &\quad + \sum_{E\in\mathcal{E}(\Gamma_D)} h_E \|(\mathbb{C}^{-1}\sigma_\ell + \operatorname{skew}(Du_\ell^*) - Du_D)\tau\|^2_{L^2(E)},\end{aligned}$$

where u_ℓ^* denotes the post-processed displacement of Section 4. Note that the unknown reliability constant of Theorem 3.6 is set to one and therefore η_ℓ possibly underestimates the error in the numerical experiments.

Mark. Based on local values $\eta_\ell(T)$ of η_ℓ and a bulk parameter $0 < \theta \leq 1$, some triangles are marked for refinement in a bulk criterion [Dör96] such that $\mathcal{M}_\ell \subseteq \mathcal{T}_\ell$ is an (almost) minimal set of elements with

$$\theta\eta_\ell^2 \leq \sum_{T\in\mathcal{M}_\ell} \eta_\ell^2(T).$$

Refine. Once an element is selected for refinement, all of its edges are marked for refinement. In a closure algorithm additional edges are

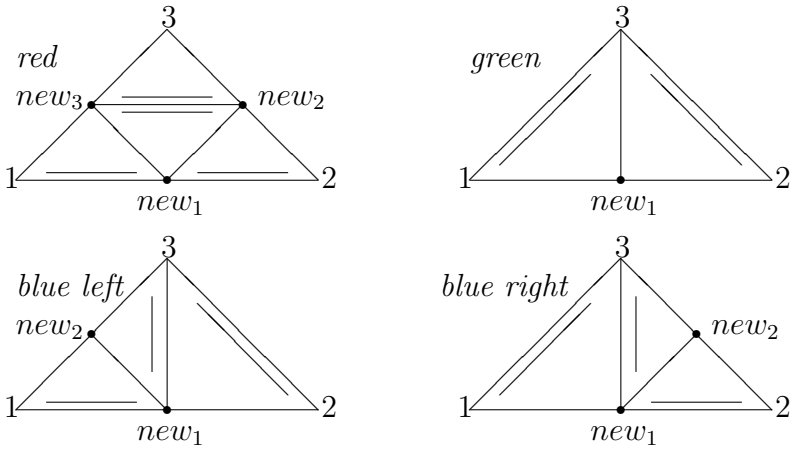

FIGURE 5.1. Refinement rules: Sub-triangles with corresponding reference edges depicted with a second edge.

marked, such that once an edge of a triangle is marked for refinement, its reference edge is marked as well. After the closure algorithm is applied, one of the following refinement rules is applicable, namely no refinement, red refinement, green refinement, blue-left or blue-right refinement depicted in Figure 5.1.

Further details and references on related adaptive finite element methods in elasticity can be found in [CFPP14] with an axiomatic approach for optimal convergence rates.

5.2. **Academic example.** Consider the model problem (1.1) on the unit square $\Omega = (0,1) \times (0,1)$ with homogeneous Dirichlet boundary conditions. The elasticity modulus is set to $E = 10^5$ and the Poisson ratio is chosen either $\nu = 0.3$ or $\nu = 0.4999$. The right-hand side reads

$$\begin{aligned} f_1(x,y) &= -2\mu\pi^3 \cos(\pi y)\sin(\pi y)(2\cos(2\pi x) - 1), \\ f_2(x,y) &= \quad 2\mu\pi^3 \cos(\pi x)\sin(\pi x)(2\cos(2\pi y) - 1), \end{aligned}$$

and depends only on the Lamé parameter μ and not on the critical Lamé parameter λ. The corresponding displacements read

$$\begin{aligned} u_1(x,y) &= \quad \pi \cos(\pi y)\sin^2(\pi x)\sin(\pi y), \\ u_2(x,y) &= -\pi \cos(\pi x)\sin(\pi x)\sin^2(\pi y). \end{aligned}$$

Uniform refinement leads to optimal convergence rates as shown in Figure 5.2. Since the solution is smooth, the proposed post-processing with third-order polynomials shows higher-order converge rates for the L^2, the energy and the error of the asymmetric part of the gradient. The a posteriori error estimator η_ℓ is an upper bound of the energy error and the oscillations of the right-hand side dominate the a posteriori error estimator in this example. Note that all the errors of the post-processed solution are independent of the Poisson ratio $\nu \to 1/2$ which verifies the robustness of the post-processing.

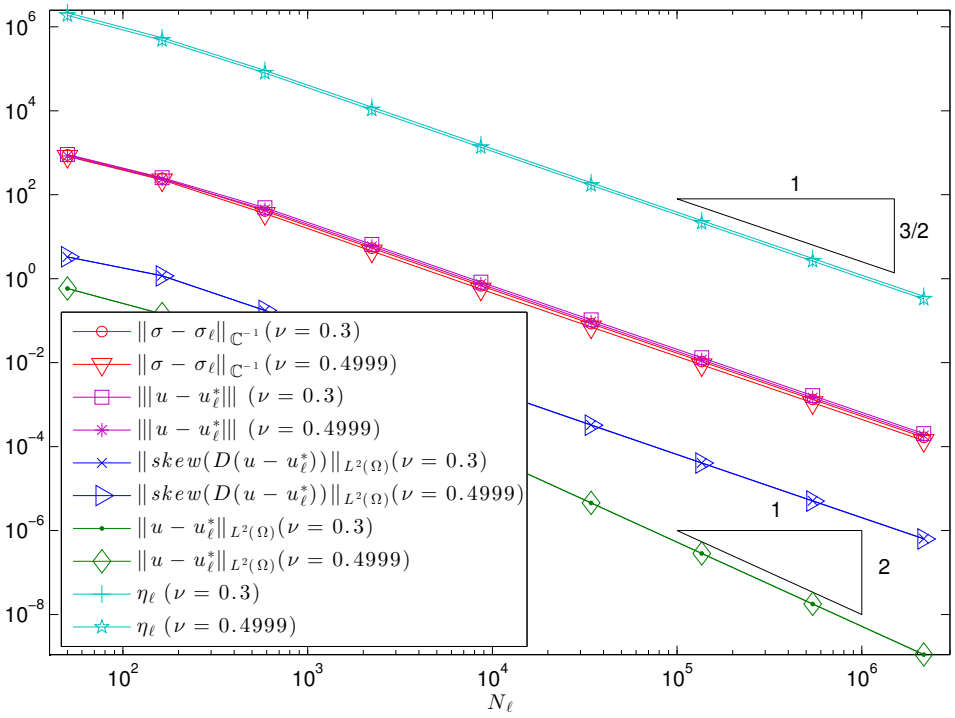

FIGURE 5.2. Convergence history with uniform and adaptive mesh-refinements for the academic example

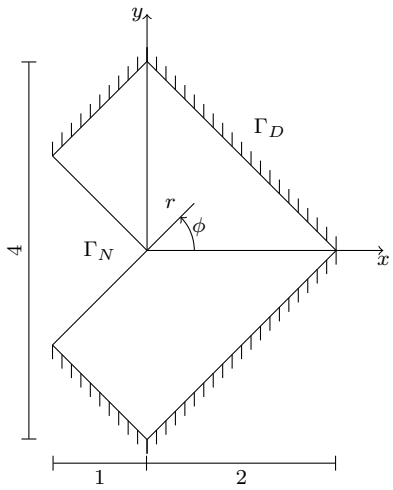

FIGURE 5.3. The L-shaped domain.

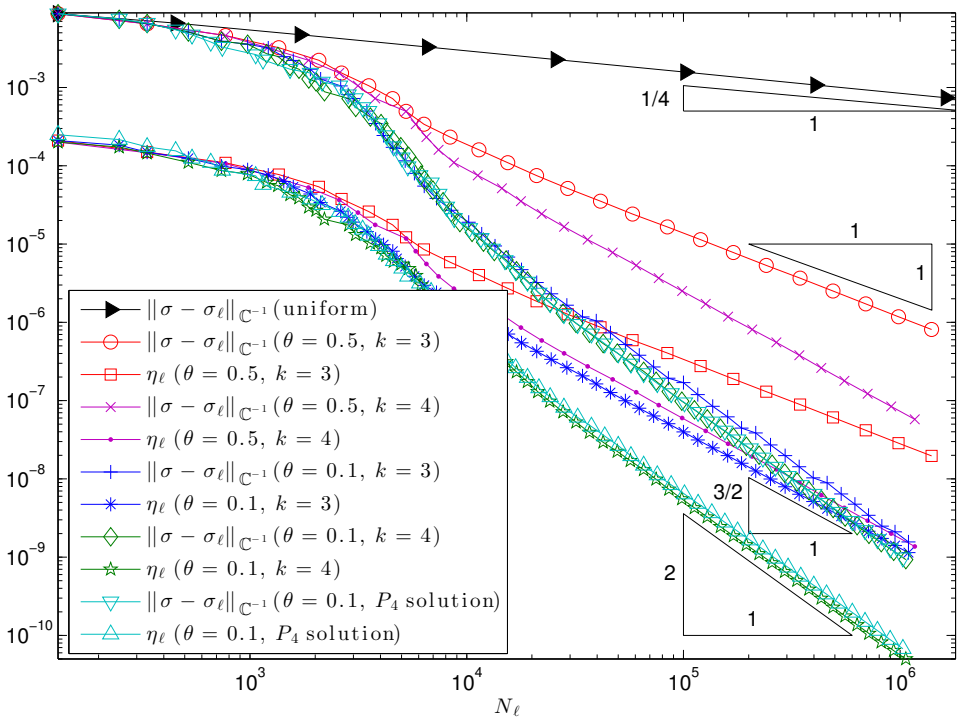

FIGURE 5.4. Convergence history with uniform and adaptive mesh-refinements for the L-shaped benchmark

5.3. **L-shaped benchmark.** The second example considers the model problem (1.1) on the rotated L-shaped domain Ω as depicted in Figure 5.3. The exact solution read in polar coordinates

$$u_r(r,\phi) = \frac{r^\alpha}{2\mu}\left(-(\alpha+1)\cos((\alpha+1)\phi) + (C_2-\alpha-1)C_1\cos((\alpha-1)\phi)\right),$$
$$u_\phi(r,\phi) = \frac{r^\alpha}{2\mu}\left((\alpha+1)\sin((\alpha+1)\phi) + (C_2+\alpha-1)C_1\sin((\alpha-1)\phi)\right).$$

The constants are $C_1 := -\cos((\alpha+1)\omega)/\cos((\alpha-1)\omega)$ and $C_2 := 2(\lambda+2\mu)/(\lambda+\mu)$, where $\alpha = 0.544483736782$ is the positive solution of $\alpha\sin(2\omega) + \sin(2\omega\alpha) = 0$ for $\omega = 3\pi/4$ and with Lamé parameter λ and μ according to the elasticity modulus $E = 10^5$ and the Poisson ratio $\nu = 0.4999$. The volume force and the Neumann boundary data vanish, and the Dirichlet boundary conditions are taken from the exact solution. The exact solution exhibits a strong singularity at the origin. Figure 5.4 shows that adaptive mesh-refinement leads to better convergence rates than uniform refinement. The convergence rate of uniform refinement is smaller than the expected rate 1/3. This loss of convergence results from the Neumann boundary condition that leads to the pre-described zero values for the nodal stress degrees of freedom in the origin. This is a particular difficulty of the Arnold–Winther finite element method. The experiments show that a bulk parameter

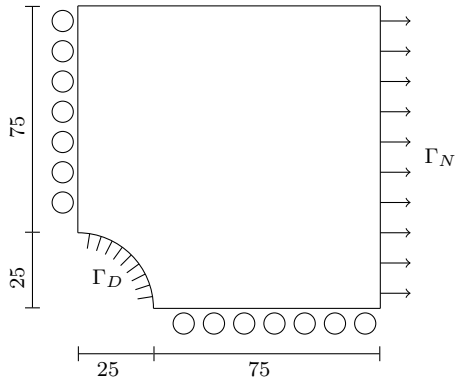

FIGURE 5.5. Domain circular inclusion.

$\theta = 0.5$ with third-order post-processing for u_ℓ^* leads to suboptimal convergence rates, while the choice of $\theta = 0.1$ leads to super-convergence of the energy error of $\mathcal{O}(\mathcal{N}_\ell^{-2})$. Note that this super-convergence phenomenon has also been observed in [CGP12, CGRT08]. In that case the third-order post-processing is not efficient. Therefore, in the following examples the polynomial degree of the post-processing is chosen to be four which leads to efficient a posteriori error estimators. The comparison of the residual-based a posteriori error estimator with fourth-order post-processing to the residual a posteriori error estimator with a conforming fourth-order displacement-based FEM shows comparable results and that the values of the estimator with post-processing are even slightly smaller.

5.4. **Circular inclusion.** A rigid circular inclusion in an infinite plate for the domain Ω is shown in Figure 5.5. The exact solution [KS95] to the model problem (1.1) in polar coordinates (r, ϕ) reads

$$u_r = \frac{1}{8\mu r}\left((\kappa-1)r^2 + 2\gamma a^2 + \left(2r^2 - \frac{2(\kappa+1)a^2}{\kappa} + \frac{2a^4}{\kappa r^2}\right)\cos(2\phi)\right),$$
$$u_\phi = -\frac{1}{8\mu r}\left(2r^2 - \frac{2(\kappa-1)a^2}{\kappa} - \frac{2a^4}{\kappa r^2}\right)\sin(2\phi),$$

where $\kappa = 3-4\nu$, $\gamma = 2\nu-1$, $a = 1/4$ and μ is the Lamé parameter determined by $E = 10^5$ and the Poisson ratio $\nu = 0.3$ or $\nu = 0.4999$. The linear boundary approximation of the circular inclusions is critical for the higher-order Arnold–Winther FEM. Theorem 3.1 and Lemma 3.3 show

$$\|\sigma - \sigma_{\mathrm{AW}}\|_{\mathbb{C}^{-1}}^2 \lesssim \mathrm{osc}^2(f, \mathcal{T}) + \mathrm{osc}^2(g, \mathcal{E}(\Gamma_N)) + \mathrm{dist}_{\mathbb{C}}^2(\mathbb{C}^{-1}\sigma_{\mathrm{AW}}, \varepsilon(u_D + V)).$$

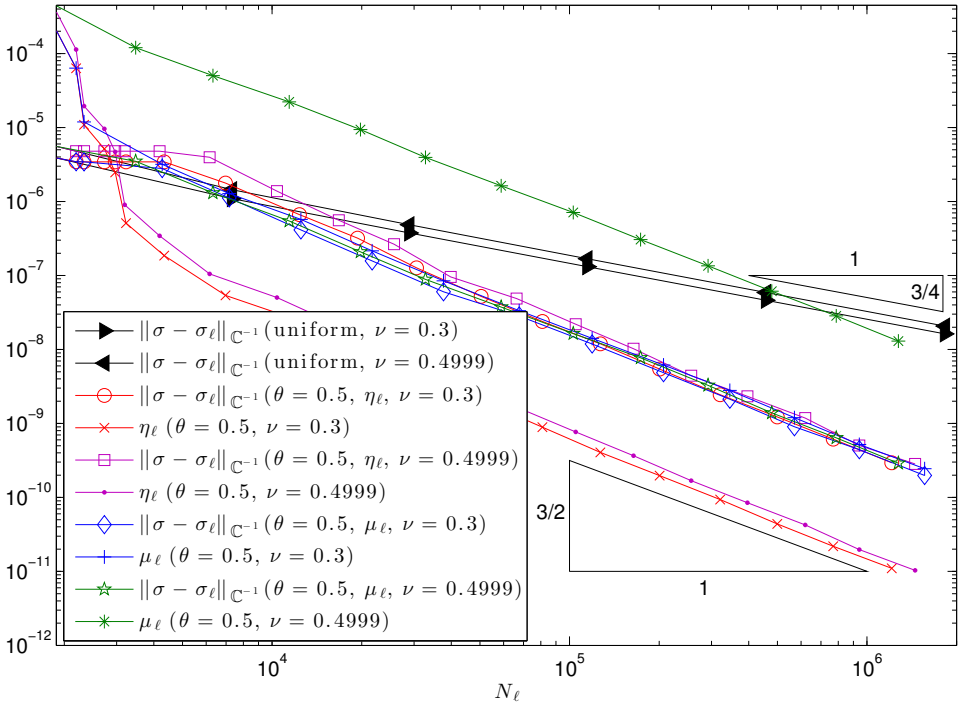

FIGURE 5.6. Convergence history with uniform and adaptive mesh-refinements for the circular inclusion domain

This gives rise to the a posteriori error estimator μ_ℓ

$$\mu_\ell^2 = \operatorname{osc}^2(f, \mathcal{T}) + \operatorname{osc}^2(g, \mathcal{E}(\Gamma_N)) + |||\mathbb{C}^{-1}\sigma_\ell - \varepsilon(\tilde{u}_\ell^*)|||^2 + \sum_{E\in\mathcal{E}_h, E\subseteq\Gamma_D} h_E \|\partial(u_D - \tilde{u}_\ell^*)/\partial s\|^2_{L^2(E)},$$

where the conforming approximation $\tilde{u}_\ell^* \in P_4(\mathcal{T}_\ell, \mathbb{R}^2)$ is obtained from the post-processed (possibly) discontinuous approximation $u_\ell^* \in P_4(\mathcal{T}_\ell, \mathbb{R}^2)$ by taking the arithmetic mean value

$$\tilde{u}_\ell^*(z) := \frac{1}{|\{T \in \mathcal{T}_h : z \in T\}|} \sum_{T\in\mathcal{T}_h : z\in T} u_\ell^*(z)|_T,$$

for each vertex and edge degree of freedom in $z \in \mathbb{R}^2$. The boundary degrees of freedom in points $z \in \mathbb{R}^2$ are interpolated $\tilde{u}_\ell^*(z) = u_D(z)$. Hence, the Dirichlet boundary conditions might not be fulfilled exactly and the last a posteriori error term of μ_ℓ controls that difference [CGP12, Remark 5.3]. Adaptive mesh-refinement leads to optimal convergence rates while uniform mesh-refinement is suboptimal (See Figure 5.6). The a posteriori error estimator η_ℓ is robust in ν while the other a posteriori error estimator μ_ℓ increases as $\nu \to 1/2$. The empirical observation is that while the discontinuous approximation u_ℓ^* is robust in ν, the averaged approximation $\tilde{u}_\ell^*$ is not. Hence, the new

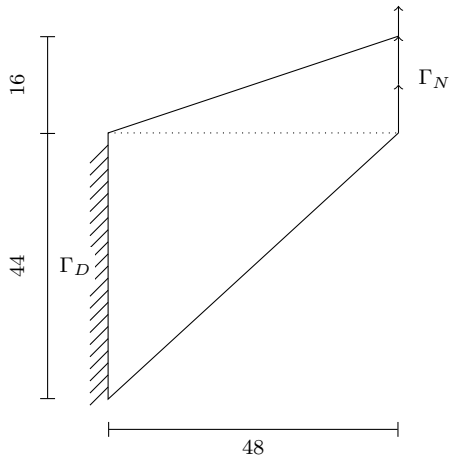

FIGURE 5.7. The Cook's membrane.

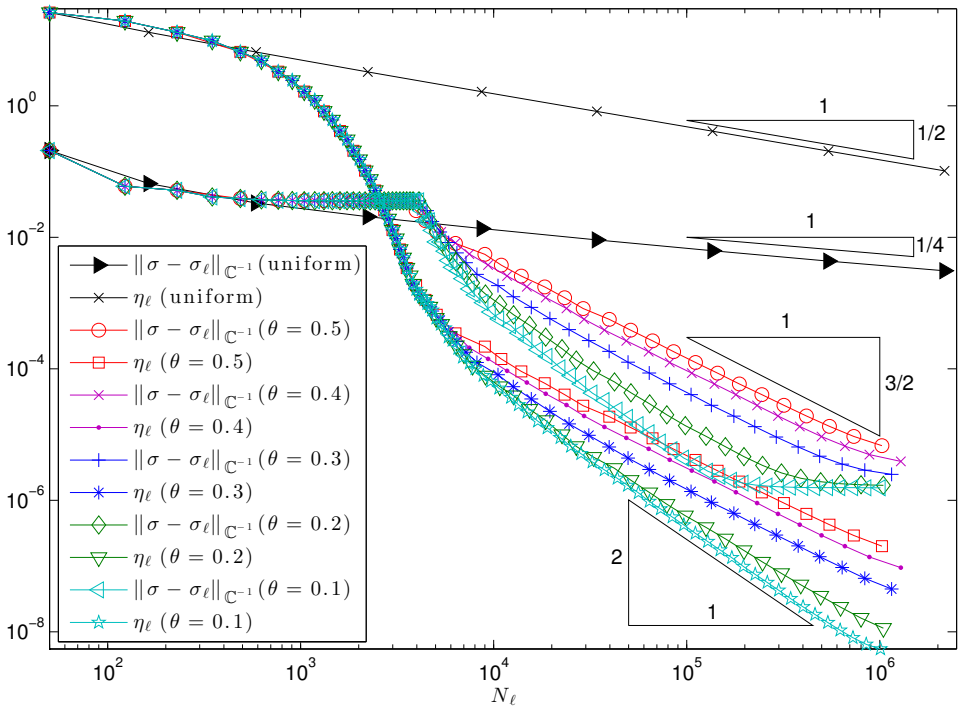

FIGURE 5.8. Convergence history with uniform and adaptive mesh-refinements for Cook's membrane

residual a posteriori error estimator η_ℓ is better for the linear elastic problem (1.1) than the a posteriori error estimator μ_ℓ.

5.5. **Cook's membrane problem.** This benchmark problem considers the model problem (1.1) with Ω depicted in Figure 5.7. The domain describes a tapered panel which is clamped on the left side and subject to a surface load in vertical direction on the right side. The interior

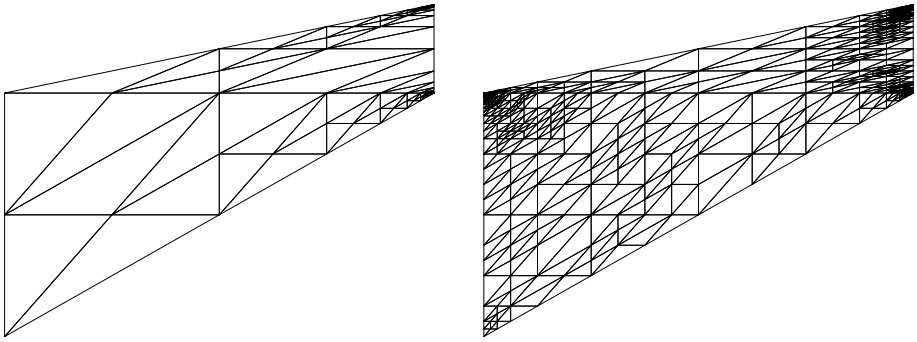

FIGURE 5.9. Adaptively refined meshes for $\theta = 0.1$ with 150 and 764 nodes for Cook's membrane

load is zero, $f \equiv 0$. For $(x, y) \in \Gamma_N$, the surface load is given by $g(x, y) = (0, 1)$ if $x = 48$ and $g(x, y) = 0$ elsewhere. Since the plate is clamped, $u_D \equiv 0$ on Γ_D. This benchmark problem is a standard test for bending dominated response. In the numerical experiments, the elasticity modulus is $E = 10^5$ and the Poisson ratio $\nu = 0.499$. This example is a particular difficult example for the Arnold–Winther MFEM because of the incompatible Neumann boundary conditions on the right corners. As described in [CGRT08] the nodal degrees of freedom in the two right corners are chosen to be a discrete least-squares fitting of the neighbouring boundary conditions. Therefore at the beginning, the Neumann boundary oscillations dominate the a posteriori error estimator while the error of the solution is governed by the singularity at the top left corner. Due to the lack of an analytic solution, the unknown energy error is approximated by a P_5 solution on the red-refinement of the last and sufficiently fine mesh. Figure 5.8 shows for uniform refinement the huge pre-asymptotic range of the a posteriori error estimator which covers the whole range of computed values while for adaptive refinement it ends around $N_\ell = 4000$. Beyond that the energy error converges and the a posteriori error estimator becomes a lower bound of the error due to the chosen value one for the unknown generic constant in the reliability estimate. The pre-asymptotic refinement in the Neumann boundary corners is illustrated in Figure 5.9 where the coarse mesh is in the pre-asymptotic regime while the fine mesh is in the range of optimal convergence. Different choices of the bulk parameter lead to different convergence rates and the choice $\theta = 0.1$ leads to the super-convergence of $\mathcal{O}(N_\ell^{-2})$. The energy error does not decrease below 10^{-6} because the accuracy of the method or the accuracy of the error approximation is reached.

REFERENCES

[AW02] D. N. Arnold and R. Winther, *Mixed finite elements for elasticity*, Numer. Math. **92** (2002), no. 3, 401–419.

[BBF13] D. Boffi, F. Brezzi, and M. Fortin, *Mixed finite element methods and applications*, second ed., Springer, Heidelberg, Cambridge, 2013.

[Bra01] D. Braess, *Finite elements*, second ed., Cambridge University Press, Cambridge, 2001, Theory, fast solvers, and applications in solid mechanics, Translated from the 1992 German edition by Larry L. Schumaker.

[Bre74] F. Brezzi, *On the existence, uniqueness and approximation of saddle-point problems arising from lagrangian multipliers*, Rev. Franc. Automat. Inform. Rech. Operat. **R-2** (1974), no. 8, 129–151.

[BS94] S.C. Brenner and L.R. Scott, *The mathematical theory of finite element methods*, Texts in Applied Mathematics, vol. 15, Springer-Verlag, New York, 1994.

[Car05] C. Carstensen, *A unifying theory of a posteriori finite element error control*, Numer. Math. **100** (2005), no. 4, 617–637.

[CD98] C. Carstensen and G. Dolzmann, *A posteriori error estimates for mixed FEM in elasticity*, Numer. Math. **81** (1998), no. 2, 187–209.

[CEG11] C. Carstensen, M. Eigel, and J. Gedicke, *Computational competition of symmetric mixed FEM in linear elasticity*, Comput. Methods Appl. Mech. Engrg. **200** (2011), no. 41-44, 2903–2915.

[CFPP14] C. Carstensen, M. Feischl, M. Page, and D. Praetorius, *Axioms of adaptivity*, Comput. Methods Appl. Math. **67** (2014), no. 6, 1195–1253.

[CGP12] C. Carstensen, J. Gedicke, and E.-J. Park, *Numerical experiments for the Arnold-Winther mixed finite elements for the Stokes problem*, SIAM J. Sci. Comput. **34** (2012), no. 4, A2267–A2287.

[CGRT08] C. Carstensen, D. Günther, J. Reininghaus, and J. Thiele, *The Arnold-Winther mixed FEM in linear elasticity. part I: Implementation and numerical verification*, Comput. Methods Appl. Mech. Engrg. **197** (2008), 3014–3023.

[CGS15] C. Carstensen, D. Gallistl, and M. Schedensack, *L^2 best-approximation of the elastic stress in the Arnold-Winther finite element method*, IMA J. Numer. Anal., published online, doi:10.1093/imanum/drv051, 2015.

[CH07] C. Carstensen and J. Hu, *A unifying theory of a posteriori error control for nonconforming finite element methods*, Numer. Math. **107** (2007), no. 3, 473–502.

[Clé75] Ph. Clément, *Approximation by finite element functions using local regularization*, RAIRO Analyse Numérique **9** (1975), no. R-2, 77–84.

[Dör96] W. Dörfler, *A convergent adaptive algorithm for Poisson's equation*, SIAM J. Numer. Anal. **33** (1996), 1106–1124.

[KS95] R. Kouhia and R. Stenberg, *A linear nonconforming finite element method for nearly incompressible elasticity and Stokes flow*, Comput. Methods Appl. Mech. Engrg. **124** (1995), no. 3, 195–212.

[LS10] R.S. Laugesen and B.A. Siudeja, *Minimizing Neumann fundamental tones of triangles: an optimal Poincaré inequality*, J. Differential Equations **249** (2010), no. 1, 118–135.

[Ste88] R. Stenberg, *A family of mixed finite elements for the elasticity problem*, Numer. Math. **53** (1988), no. 5, 513–538.

[Ver94] R. Verfürth, *A posteriori error estimation and adaptive mesh-refinement techniques*, J. Comput. Appl. Math. **50** (1994), no. 1-3, 67–83.

[Ver96] R. Verfürth, *A review of a posteriori error estimation and adaptive mesh-refinement techniques*, Wiley and Teubner, 1996.

[Vog83] Michael Vogelius, *An analysis of the p-version of the finite element method for nearly incompressible materials*, Numer. Math. **41** (1983), no. 1, 39–53.

(C. Carstensen) Institut für Mathematik, Humboldt-Universität zu Berlin, Unter den Linden 6, 10099 Berlin, Germany
E-mail address: cc@mathematik.hu-berlin.de

(J. Gedicke) Interdisziplinäres Zentrum für Wissenschaftliches Rechnen (IWR), Universität Heidelberg, Im Neuenheimer Feld 368, 69120 Heidelberg, Germany
E-mail address: joscha.gedicke@iwr.uni-heidelberg.de